

AD \_\_\_\_\_

Grant Number DAMD17-96-1-6131

TITLE: Vascular Functional Imaging and Physiological Environment  
of Hyperplasia, Non-Metastatic and Metastatic Breast Cancer

PRINCIPAL INVESTIGATOR: Zaver M. Bhujwalla, Ph.D.

CONTRACTING ORGANIZATION: The Johns Hopkins University  
Baltimore, Maryland 21205-5014

REPORT DATE: October 1998

TYPE OF REPORT: Annual

PREPARED FOR: U.S. Army Medical Research and Materiel Command  
Fort Detrick, Maryland 21702-5012

DISTRIBUTION STATEMENT: Approved for public release;  
distribution unlimited

The views, opinions and/or findings contained in this report are  
those of the author(s) and should not be construed as an official  
Department of the Army position, policy or decision unless so  
designated by other documentation.

19990407 078

# REPORT DOCUMENTATION PAGE

Form Approved  
OMB No. 0704-0188

Public reporting burden for this collection of information is estimated to average 1 hour per response, including the time for reviewing instructions, searching existing data sources, gathering and maintaining the data needed, and completing and reviewing the collection of information. Send comments regarding this burden estimate or any other aspect of this collection of information, including suggestions for reducing this burden, to Washington Headquarters Services, Directorate for Information Operations and Reports, 1215 Jefferson Davis Highway, Suite 1204, Arlington, VA 22202-4302, and to the Office of Management and Budget, Paperwork Reduction Project (0704-0188), Washington, DC 20503.

<b>1. AGENCY USE ONLY (Leave blank)</b>		<b>2. REPORT DATE</b> October 1998	<b>3. REPORT TYPE AND DATES COVERED</b> Annual (1 Oct 97 - 30 Sep 98)	
<b>4. TITLE AND SUBTITLE</b> Vascular Functional Imaging and Physiological Environment of Hyperplasia, Non-Metastatic and Metastatic Breast Cancer			<b>5. FUNDING NUMBERS</b> DAMD17-96-1-6131	
<b>6. AUTHOR(S)</b> Zaver M. Bhujwalla, Ph.D.				
<b>7. PERFORMING ORGANIZATION NAME(S) AND ADDRESS(ES)</b> The Johns Hopkins University Baltimore, MD 21205-5014			<b>8. PERFORMING ORGANIZATION REPORT NUMBER</b>	
<b>9. SPONSORING/MONITORING AGENCY NAME(S) AND ADDRESS(ES)</b> Commander U.S. Army Medical Research and Materiel Command Fort Detrick, Frederick, Maryland 21702-5012			<b>10. SPONSORING/MONITORING AGENCY REPORT NUMBER</b>	
<b>11. SUPPLEMENTARY NOTES</b>				
<b>12a. DISTRIBUTION / AVAILABILITY STATEMENT</b> Approved for public release; distribution unlimited			<b>12b. DISTRIBUTION CODE</b>	
<b>13. ABSTRACT (Maximum 200)</b>  Our research proposal consists of the following three closely related aims directed towards understanding the role of vascular, physiological and metabolic properties in the metastatic dissemination of breast cancer. Aim 1: To investigate the relationship between metastatic phenotype and vascularization. Aim 2: To investigate the effect of increasing vascularization and permeability on metastasis. Aim 3: To determine the relationship between metastatic phenotype and intra- and extracellular pH and lactate production. In year 2 we have implemented significant technical developments which allow us to interactively display and correlate 3-dimensional MRI information of vascular volume and permeability with 3D reconstructed histological maps. These developments, instead of the single slice data acquisition we originally proposed, have allowed us to obtain comprehensive information of tumor vascular volume and permeability as well as histological morphology and the relationship between the tow. We have also characterized the metabolism of human mammary epithelial cells (HMEC) and demonstrated for the first time that HMEC show significantly altered lactate levels and phospholipid metabolism with malignancy.				
<b>14. SUBJECT TERMS</b> Breast Cancer			<b>15. NUMBER OF PAGES</b> 21	
			<b>16. PRICE CODE</b>	
<b>17. SECURITY CLASSIFICATION OF REPORT</b> Unclassified	<b>18. SECURITY CLASSIFICATION OF THIS PAGE</b> Unclassified	<b>19. SECURITY CLASSIFICATION OF ABSTRACT</b> Unclassified	<b>20. LIMITATION OF ABSTRACT</b> Unlimited	

## FOREWORD

Opinions, interpretations, conclusions and recommendations are those of the author and are not necessarily endorsed by the U.S. Army.

\_\_\_\_ Where copyrighted material is quoted, permission has been obtained to use such material.

\_\_\_\_ Where material from documents designated for limited distribution is quoted, permission has been obtained to use the material.

\_\_\_\_ Citations of commercial organizations and trade names in this report do not constitute an official Department of Army endorsement or approval of the products or services of these organizations.


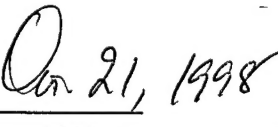
✓ \_\_\_\_ In conducting research using animals, the investigator(s) adhered to the "Guide for the Care and Use of Laboratory Animals," prepared by the Committee on Care and use of Laboratory Animals of the Institute of Laboratory Resources, national Research Council (NIH Publication No. 86-23, Revised 1985).

✓ \_\_\_\_ For the protection of human subjects, the investigator(s) adhered to policies of applicable Federal Law 45 CFR 46.

\_\_\_\_ In conducting research utilizing recombinant DNA technology, the investigator(s) adhered to current guidelines promulgated by the National Institutes of Health.

\_\_\_\_ In the conduct of research utilizing recombinant DNA, the investigator(s) adhered to the NIH Guidelines for Research Involving Recombinant DNA Molecules.

\_\_\_\_ In the conduct of research involving hazardous organisms, the investigator(s) adhered to the CDC-NIH Guide for Biosafety in Microbiological and Biomedical Laboratories.

   
PI - Signature Date

## **TABLE OF CONTENTS**

	<b><u>Page No.</u></b>
1. FRONT COVER	1
2. STANDARD FORM (SF) 298, REPORT DOCUMENTATION PAGE	2
3. FOREWORD	3
4. TABLE OF CONTENTS	4
5. INTRODUCTION	5
6. BODY	
STUDY 1. EXPERIMENTAL METHODS	7
RESULTS AND DISCUSSION	9
STUDY 2. EXPERIMENTAL METHODS	14
RESULTS AND DISCUSSION	15
7. CONCLUSIONS	17
8. REFERENCES	18

## **INTRODUCTION**

Vascularization plays a key role in the growth and metastasis of solid tumors [1-6]. In two recent clinical studies, breast cancer patients whose tumors had a high vascular density subsequently went on to develop metastases over a follow up period of 2.5 years [7, 8]. Statistical analyses of these patients showed that vascular density was the single most important factor ( $p < 0.006$ ) associated with subsequent formation of metastasis [8]; the other factors examined were epidermal growth factor receptor status ( $p < 0.01$ ), node status ( $p < 0.02$ ), estrogen receptor status ( $p < 0.05$ ), tumor size ( $p < 0.06$ ), tumor grade ( $p < 0.5$ ), c-erb-2 expression ( $p < 0.7$ ), p53 ( $p < 0.8$ ) and tumor type ( $p < 0.8$ ). Studies correlating vascularization with metastasis have so far been performed with histological evaluation of excised tissue specimens [7, 8] as a result of which information regarding functioning of vessels is lost. Similarly, the physiological environment of these tumors, in terms of acidity and lactate production remains unknown. Thus a lack of noninvasive methods has left some vital questions about the precise nature of the relationship between vascularization and metastasis unanswered. Tumor neovascularization is induced by the secretion of angiogenic factors which act as chemotactic factors and mitogens for endothelial cells [1, 4-6]. One of the most potent of these is vascular endothelial growth factor (VEGF). VEGF also increases vascular permeability which in turn may allow cancer cells greater access to the vasculature [9]. In glioblastoma multiforme areas of necrosis and hypoxia show a higher expression of VEGF [10, 11]. Poorly functioning vessels and the associated hypoxia and necrosis may play a role in attracting further vascularization. Areas of hypoxia are also associated with accumulation of lactate and low pH. These two physiological factors attract neovascularization by stimulating the secretion of angiogenic factors from macrophages [12-15]. The secretion of enzymes which degrade the basement membrane in the metastatic process increases at low pH [16, 17]. Thus, vascularization, the physiological environment, and formation of metastases are highly interdependent. An understanding of the role of the physiological environment in vascularization and metastasis, and the dependence of this environment on metastatic phenotype are essential to delineate the relationship between vascularization and metastasis. Questions which are central to understanding this relationship are - (1) does the metastatic phenotype induce a higher degree of vascularization and is this mediated by modulation of the physiological environment? (addressed in Specific Aims 1 and 3) (2) If so, do nonmetastatic tumors and preneoplastic tissue exhibit proportionately lower vascularization? (addressed in Specific Aims 1 and 2) (3) Which particular property of the vascularization e.g. permeability, volume or relative perfusion is the dominant factor in the dependence of metastasis on vascularization? (addressed in Specific Aims 1 and 2) (4) Is a significant fraction of the vessels observed in the histological studies non-functional and does the resultant unsuitable environment induce expression of signals or substances which prompt and enable the cells to metastasize? (addressed in Specific Aim 1). The overall goal of this research proposal is to use noninvasive Magnetic Resonance (MR) Imaging (I) and Spectroscopy (S) to answer the questions posed above.

The research proposed consists of three closely related aims designed to unravel the complex relationship between vascularization and metastasis. Our overall goal in this project is to determine key vascular and physiological properties which result in the close

relationship between vascular density and metastasis as this information may ultimately be used to prevent tumor metastasis. We had proposed the following three aims:

Aim 1: To investigate the relationship between metastatic phenotype and the development of vascularization and evaluate the functionality of the developing vascularization in terms of vascular volume, vascular permeability and relative perfusion.

Hypothesis #1: More metastatic lines will exhibit a higher level of vascularization and permeability for similar volumes. A significant number of vessels detected by immunoperoxidase staining will not be functional and this number will increase with the size of the tumor.

Aim 2: To investigate the effect of increasing (a) tumor vascularization and (b) tumor vascularization and permeability on the formation of metastases.

Hypothesis #2: Higher vascularization and permeability will lead to an increase or an earlier incidence of metastases for all the lines.

(Aims 1 and 2 are related to questions 1-4 outlined in background)

Aim 3: To determine the relationship between metastatic phenotype and intra- and extracellular pH and lactate production.

Hypothesis #3: More metastatic lines will be more glycolytically active *in vivo*, creating an environment of high lactate and low extracellular pH for volume matched lesions.

(Aim 3 is related to question 1 outlined in background)

Last year we presented data which demonstrated that there were significant differences in the vascular volume generated by a invasive metastatic human breast cancer line MDA-MB-231 and a nonmetastatic cancer line RIF-1. Studies correlating VEGF distribution with MRI maps of vascular volume and permeability demonstrated that areas around necrosis showed high expression of VEGF and were more permeable. We also presented data to demonstrate that there were significant differences in pH regulation and the phospholipid metabolism in solid tumors growing *in vivo* in SCID mice for a highly metastatic and a less metastatic human breast cancer line. We had therefore made significant progress in Aim 1 and Aim 3 by the end of the first year of the grant.

The technical objectives outlined in our statement of work continue to remain the same and these are: Delineate the role of vascular volume, permeability and perfusion and tumor physiological environment in the formation of metastasis from human breast cancer lines with preselected invasive and metastatic potential grown in SCID (severe combined immune deficient) mice.

In our original statement of work we had proposed investigating the immortalized human breast line MCF12A and the three human breast cancer lines MCF-7, MDA-MB-231 and MDA-MB-435. While characterizing the metabolism of these four human breast cell lines it became very apparent that there were obvious and highly significant differences in lactate levels and phospholipids between the immortalized MCF12A breast line that we had proposed using and the invasive metastatic breast cancer lines. We were therefore compelled to extend these important findings to a range of human mammary epithelial

cells progressing from normal human mammary epithelial cells obtained from reduction mammoplasty to highly invasive metastatic breast cancer lines since these findings would be extremely useful for diagnosis, prognosis as well as new therapeutic approaches. Several of these lines are derived from normal tissue and therefore will not grow in SCID mice. We therefore studied all the lines in culture to enable a quantitative comparison across the lines. Although these studies required an effort over and above what we had anticipated we were rewarded in that we have now demonstrated conclusively and for the first time that human mammary cells undergo a significant alteration in phospholipid metabolism and lactate production as they progress towards malignancy. A major part of these observations has been accepted for publication as a full length article in Cancer Research.

During the course of our vascularization studies we also realized that the single slice image acquisition protocol we had proposed where vascular volume and permeability were obtained from a single slice through the center of the tumor did not provide a comprehensive measure of tumor vascular volume and permeability. We therefore switched to acquiring multi-slice imaging data. We now acquire eight slices through the tumor. We also realized during the course of our studies last year that it was essential to obtain multi slice histological information of cellular morphology and VEGF staining and obtain 3D reconstructed maps of this histological information. This approach was therefore implemented this year in collaboration with a software expert. The software which was developed to fulfill these requirements has two novel features - (1) The software is interactive and therefore the information contained in a region of interest in the 3D MRI maps is interactively displayed in the 3D histological maps and (2) We digitize the information at high resolution and stitch the tiles together so that it is possible to zoom into regions of interest and determine the histological information in these regions of interest at a microscopic resolution. This technical development has fulfilled two goals - (1) It has allowed us to obtain comprehensive histological information of VEGF staining and histological structure and (2) The interactive nature of the software minimizes problems associated with accurate spatial co-registration for the single slice data. The acquisition of multi-slice imaging (8 slices per tumor) and histological data and the 3D reconstruction of these data sets has resulted, however, in a much more labor intensive and time consuming approach in the experimental studies. Therefore, although we have acquired most of the data to evaluate Aim 1 we are currently in the process of analyzing the results. We have, however, evaluated Aim 3 and therefore are on track in evaluating the overall technical objectives outlined in the statement of work.

Results in year two were obtained using experimental designs and techniques which apply to the individual aims (as in our research proposal). Therefore the experimental methods results and discussion are described in separate sections.

## STUDY 1. CHARACTERIZATION OF LACTATE PRODUCTION AND METABOLISM OF HUMAN BREAST CELLS

### EXPERIMENTAL METHODS

**Cell lines.** Human mammary epithelial cells (HMEC) used in this study include finite lifespan HMEC strains 184 and 48, derived from reduction mammoplasty tissues; non-tumorigenic immortal cell lines, 184A1 and 184B5, derived from benzo(a)pyrene treated 184 cells; and the 184B5-*erbB2* cell line, derived from 184B5 by transfection with the *erbB2* oncogene. All of the above cell lines were obtained from Dr. Martha Stampfer (Lawrence Berkeley National Laboratory, Berkeley, C.A.), and cultured in MCDB 170 media supplemented as previously described (21, 22). MCF-12A, a spontaneously immortalized cell line established from MCF-12M mortal cells (23), was obtained from American Type Culture Collection (Rockville, MD) and cultured in DMEM-Ham's F12 medium supplemented as previously described (23). All the human breast cancer cell lines were derived from pleural effusions in patients with breast cancer and were obtained from American Type Culture Collection (Rockville, MD). The tumor derived cell lines were all cultured in DMEM-Ham's F12 medium supplemented with 10% fetal bovine serum.

**Growth rate and cell size.** The growth rate of the cell lines used in this study were determined using the MTT assay [18]. Briefly, cells ( $5 \times 10^3$ ) were plated in 24 well plates in 1 ml of media and incubated under normal culture conditions for 6 days. To estimate cell number, the cells were incubated with MTT (Sigma, St. Louis, MO) for 4 hr. MTT was then removed and the resulting formazan crystals were dissolved in 1 ml DMSO and 125 ml glycine buffer (pH 10.5) [18]. The U.V. absorbance of the formazan solution was recorded at 553 nm ( $\lambda_{max}$ ). Four replicates were used to calculate the cell doubling time for each cell line. Since the cells had different morphologies and diameters, the cell size was determined for each cell line by trypsinizing the cells and counting the diameter of 20 random cells using an optical microscope.

**Extraction.** To determine metabolite levels, cells growing in culture were fed with fresh media 24 hr prior to extraction and used at 70-80% confluency. Cells ( $10^7$  to  $10^8$ ) were trypsinized, washed twice with normal saline and homogenized with ice cold 8% perchloric acid (5 ml). The homogenates were centrifuged (15000 rpm for 15 min at 4°C) and the supernatants neutralized with 3M  $K_2CO_3$ /1M KOH buffer. The samples were again clarified by centrifugation, treated with ~ 50 mg chelex (Sigma, St. Louis, MO) to remove divalent ions, lyophilized and resuspended in 0.5 ml of  $D_2O$  for NMR analysis. Trimethylsilyl propionate (5 ml) was used as an internal standard.  $^1H$  NMR spectra of the extracts were acquired on a 11.7T Bruker NMR spectrometer with a 5 mm probe. Fully relaxed spectra (without saturation effects) were obtained using the following acquisition parameters: 30° flip angle, 6000 Hz sweep width, 4.7 sec repetition time, 32 K block size and 512 scans. The data were analyzed using an in-house software, Soft Fourier Transform (P. Barker, The Johns Hopkins University, Baltimore, MD). Lactate, phosphocholine (PCho), glycerophosphocholine (GPC) and total choline-containing (PCho + GPC + choline) metabolite levels were determined and normalized to cell size. Between three and five independent extracts were analyzed per cell line.

The reason for normalizing metabolite levels to cell size was due to differences in cell size between the cell lines used in this study. This necessitated normalization to either cell size or protein concentration. The former requires less cells and is therefore suited to

experiments with mortal cells which senesce after a few passages and also avoids the potential problems resulting from cancer cells containing different levels of protein content compared to normal cells. To determine concentrations, peak amplitudes for lactate, choline PCho, GPC, and total choline-containing metabolites (PCho + GPC + choline) were compared to that of the internal standard trimethylsilylpropionate (TSP) according to the equation:

$$[\text{metabolite}] = \text{Amplitude}(\text{metabolite}) \times [\text{TSP}] / \{ \text{Amplitude}(\text{TSP}) \times \text{cell number} \times \text{cell volume} \}$$

...Eqn. 1.

where, [metabolite] is concentration of the metabolite expressed as fmol/ $\mu\text{m}^3$ , [TSP] is the molar concentration of TSP used, and cell volume ( $\mu\text{m}^3$ ) was calculated from the radius of the cell according to the equation, volume =  $4/3 \times \pi r^3$ . For eqn. 1 to be valid, it is necessary that spectra are fully relaxed as was the case here or to correct for saturation.

**Statistical analysis.** Statistical analysis of the data was performed using StatView II version 1.04, 1991 (Abacus Concepts, Inc., Berkeley, CA, USA). The statistical significance of differences in metabolite levels between cell lines was determined using the Mann-Whitney U test. *P* values of  $\leq 0.05$  were considered to be significant.

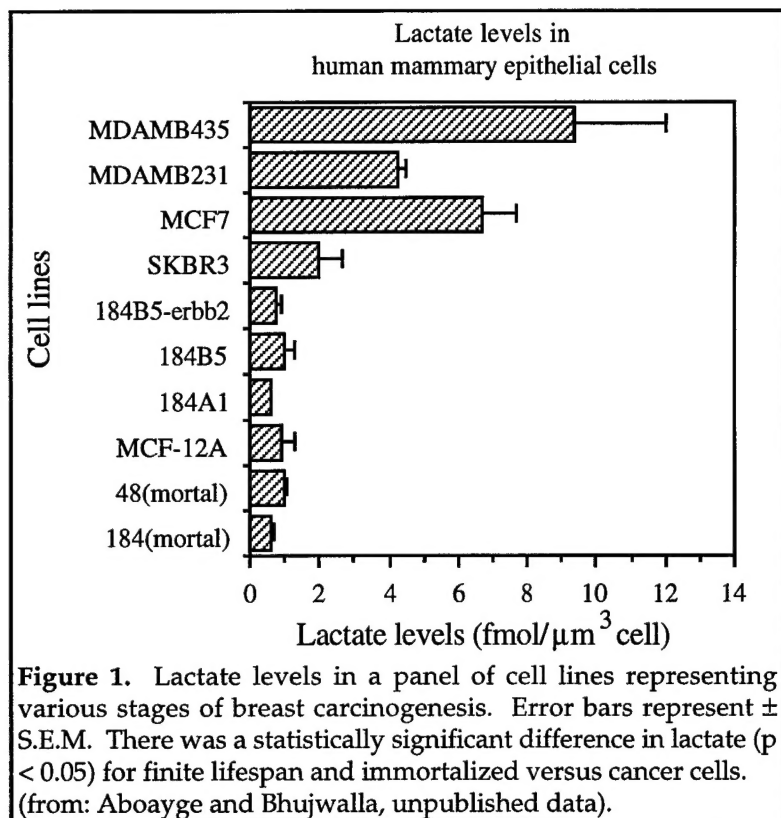
## RESULTS AND DISCUSSION

The results obtained from the experimental studies described above are presented in this section. The cell volumes and anchorage dependence of HMEC are presented in Table 1. Lactate levels obtained for these cell lines are shown in Figure 1.

Table 1: Cell volumes and anchorage dependence of HMEC (from Aboagye and Bhujwalla, Cancer Research, in press, 1998)

Cell Type	Phenotype	Cell Volume ( $\times 10^3 \text{ mm}^3$ )
<u>Normal Human mammary epithelial cells (HMEC)</u>		
184	Senescent, ADG $\P$	$6.5 \pm 6.8^{\S}$
48	Senescent, ADG	$11.1 \pm 3.1$
<u>Spontaneously immortalized HMEC</u>		
MCF-12A	Immortal, ADG	$9.8 \pm 1.8$
<u>Benzo(a)pyrene immortalized HMEC</u>		
184A1	Immortal, ADG	$7.1 \pm 0.9$
184B5	Immortal, ADG	$7.7 \pm 0.9$
<u>Oncogene-transformed HMEC</u>		
184B5-erbB2	Immortal, AIG $\dagger$ , forms low frequency, high latency tumors	$7.0 \pm 0.8$
<u>Breast Cancer Cells</u>		
SKBR3	AIG, tumorigenic, lowly metastatic	$21.9 \pm 7.3$
MCF7	AIG, tumorigenic, lowly metastatic	$8.4 \pm 1.4$
MDA-MB-231	AIG, tumorigenic, highly metastatic	$6.7 \pm 1.5$
MDA-MB-435	AIG, tumorigenic, highly metastatic	$3.5 \pm 0.4$

$\S$  Mean  $\pm$  s.e.     $\P$  ADG, Anchorage-dependent growth     $\dagger$  AIG, Anchorage-independent growth



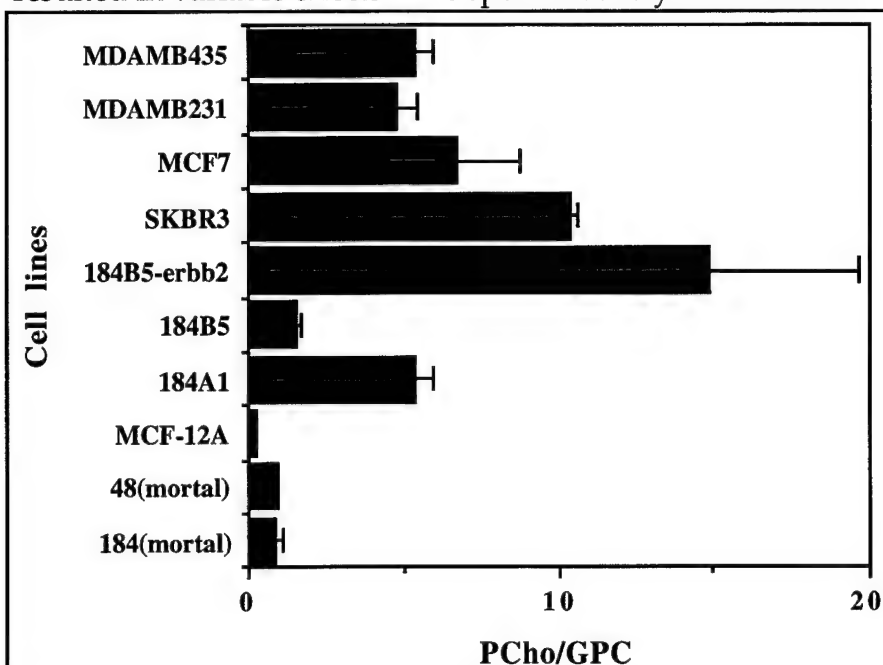
The data obtained in Figure 1 demonstrate that lactate levels are significantly higher for human breast cancer cells. Recently Schwickert et al [19] have found that patients with cervical cancers containing high lactate had a high risk of metastases. Two possible explanations for this finding are (1) A high glycolytic rate increases vascularization and is part of the invasive phenotype or (2) High lactate is indicative of anoxia and deprivation which stimulates or promotes metastasis. Supporting the latter possibility are observations that glucose starvation, acidosis and hypoxia enhance the metastatic potential of murine tumor cells [20, 21]. However, the results we have

obtained during the course of our studies demonstrate that malignant cells lines produce significantly higher levels of lactate (see Fig. 1) and support the possibility that high lactate levels are a metabolic characteristic of breast cancer cells. The increased lactate levels accompanied malignant transformation but did not appear to increase with increased metastatic potential of the breast cancer cell lines. High levels of lactate may result in a lower extracellular pH within the tumor environment which may in turn promote invasion and metastasis. For instance, Kato et al [17] have observed that two human melanoma cell lines secreted a higher level of 90-kDa gelatinase (a type IV collagenase) at an extra cellular pH of 6.8 compared to pH 7.3. This acid-induced secretion of gelatinase was blocked by cycloheximide, indicating that enzyme induction was due to *de novo* synthesis. More recently, Rozhin et al [16] have observed that an acidic pericellular pH induced a redistribution of cathepsin B+ vesicles towards the cell periphery for MCF-10 human breast parental epithelial cells and a malignantly transformed line (neoT) obtained from the parental line. For the more malignant cells this resulted in an enhanced secretion of the active form of the lysosomal protease cathepsin B over time. The results obtained here are also consistent with data we presented in our report last year demonstrating the occurrence of significantly lower extracellular pH in more metastatic breast tumor models.

#### The "GPC to PCho switch" in mammary epithelial cells.

Analysis of individual choline metabolites uncovered an early alteration in membrane choline phospholipid metabolism (MCPM) which was linked to immortalization and malignant transformation - the "GPC to PCho switch" (Fig. 2). In Fig. 2 it is evident that GPC was the major choline metabolite in the finite lifespan HMEC strains 48 and 184.

Thus, these cells showed a low PCho/GPC ratio of  $< 1$ . Immortalization of cells, however, resulted in variable effects. The spontaneously immortalized cell line MCF-12A originally



**Figure 2:** PCho/GPC ratios in a panel of cell lines representing various stages of breast carcinogenesis. Error bars represent  $\pm$  S.E.M. There was a statistically significant difference in PCho/GPC ratio ( $p < 0.05$ ) between finite lifespan versus tumor-derived cells, 184 strain versus 184A1 cell line, and 184B5 versus 184B5-*erbB2*. cell lines. The P value for 184 strain versus 184B5 cell line was 0.1 (from: Aboagye and Bhujwalla, Cancer Research, in press).

obtained from reduction mammoplasty showed a similar phenotype (PCho/GPC) as the finite lifespan cells; we do not have the finite lifespan cells from which MCF-12A was established for comparison. In contrast, the benzo(a)pyrene immortalized cell lines showed a "GPC to PCho switch", i.e. PCho was now the major choline metabolite. Of interest, the two immortal lines derived from the 184 strain showed variable degrees of this altered MCPM; 184A1 had a higher PCho/GPC level compared to 184B5.

Forced overexpression of normal *erbB2* gene into 184B5 cells dramatically increased the PCho/GPC ratio in this cell line. The altered GPC to PCho switch was detected in all breast cancer cell lines analyzed. The spectra shown in Figure 3 demonstrate the differences in GPC and PCho levels for the MCF12A human breast cells and the metastatic MDA-MB-231 human breast cancer cell line.

### Breast cancer cells have a high choline content.

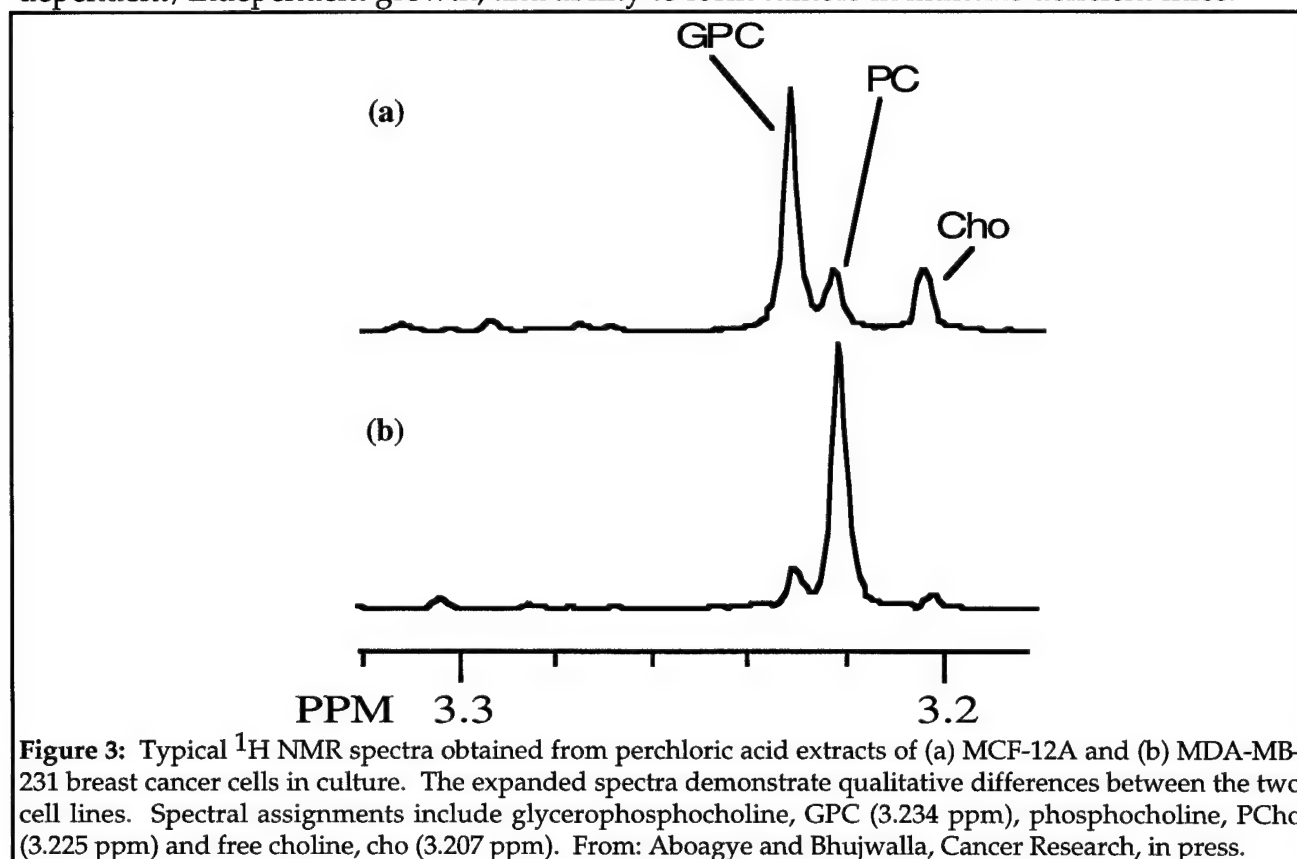
Figure 4 shows that there was a gradual increase in both PCho levels and total choline-containing metabolite levels as cells progressed from normal to malignant phenotype (normal  $<$  immortal  $<$  oncogene transformed  $<$  tumor derived). GPC levels also increased, albeit to a lesser extent than PCho levels and total choline-containing metabolite levels. It is worth noting that despite the GPC to PCho switch, total choline-containing metabolite levels and PCho levels in immortalized cell lines such as 184A1, which was non-tumorigenic, and 184B5-*erbB2*, which was lowly tumorigenic, were significantly lower than any of the tumorigenic breast cancer cells.

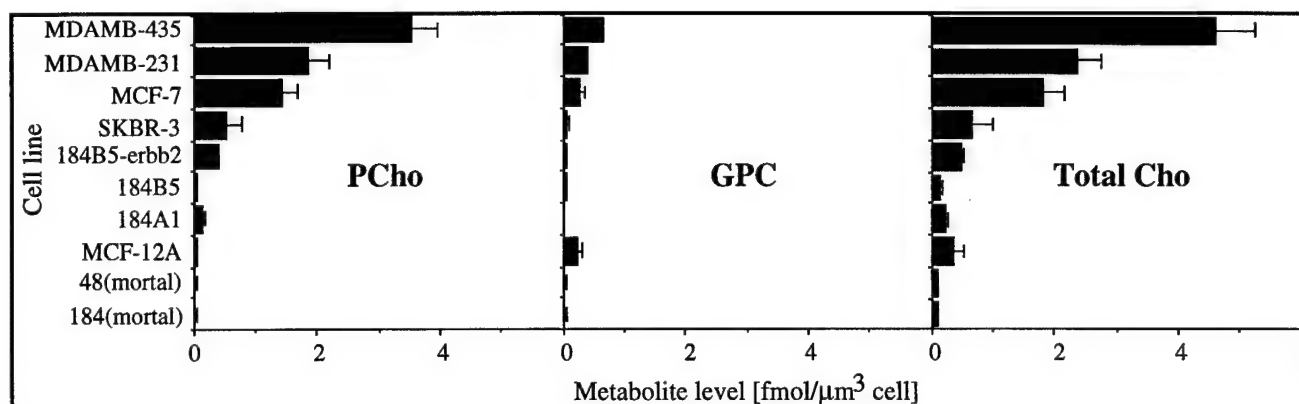
### Are the high choline phospholipid metabolite levels in breast cancer cells a function of their rate of cellular proliferation?

It is generally thought that the increase in phosphomonoester (mainly PCho and phosphoethanolamine) metabolite levels in cancer cells is due to their intensified cell membrane synthesis to cope with rapid growth and proliferation [22, 23]. This assertion is

supported, for instance, by the work of Smith *et al.*, [24], where increase in PCho and decrease in GPC correlated strongly with tumor growth rate. Thus, we tested the hypothesis that increased PCho/GPC levels, PCho, GPC or total-choline containing metabolite levels may be the result of high proliferation. A systematic measurement of cell doubling time in all the cell lines revealed that there was no overall correlation between cell doubling time and PCho/GPC ratio, PCho levels, GPC levels or total choline-containing metabolite levels. For instance MCF-12A cells exhibited a doubling time in culture comparable to the tumorigenic cell line MDA-MB-435. However, MCF-12A cells exhibited a significantly lower PCho/GPC ratio, a low level of total choline-containing metabolites and low PCho compared to MDA-MB-435 cells.

Carcinogenesis of the mammary epithelium occurs through a multistep process involving genetic alterations, amplification of oncogenes and loss of tumor suppressor function [25, 26]. The stages of carcinogenesis can broadly be classified as transformation of normal cells to benign hyperplasia followed by atypical hyperplasia which progresses to carcinoma *in situ* and finally to infiltrating carcinoma with or without metastasis to distant sites. *In vitro* models based on immortalization and oncogene transformation of normal HMEC have been developed to study mammary carcinogenesis [27-29]. These immortalized, oncogene transformed and cancer cells show differences in phenotypes that differentiate normal cells from immortal/malignant cells such as karyotype, vimentin/uvomorulin expression, responsiveness to TGF- $\beta$ , telomere length/telomerase expression, activating protein 1 transcription factor activity, as well as anchorage-dependent/independent growth, and ability to form tumors in immune deficient mice.





**Figure 4:** Phosphocholine (PCho), glycerophosphocholine (GPC) and total choline-containing metabolite (phosphocholine + glycerophosphocholine + choline) levels in a panel of cell lines representing various stages of breast carcinogenesis. Error bars represent  $\pm$  S.E.M. From: Aboagye and Bhujwalla, Cancer Research, in press.

We have investigated the association between malignant carcinogenic processes and MCPM, by monitoring the three choline phospholipid metabolites (choline, PCho and GPC) in ten cell lines which represent different stages of malignant progression. Our findings suggest that normal human mammary epithelium has low steady state levels of total choline-containing metabolites. In addition to their low total choline-containing metabolite levels, we also demonstrated that GPC was the major metabolite in the normal HMEC. A GPC to PCho switch appeared to be an early phenotypic change during carcinogenesis as observed in benzo(a)pyrene immortalized cells and where instead of GPC, PCho became the major choline phospholipid metabolites. However, despite this 'switch', total choline-containing metabolite levels remained low in these immortalized cells. Transformation of 184B5 immortal cells by forced overexpression of the *erbB2* oncogene, however, resulted in a dramatic increase in both PCho/GPC ratio and total choline levels compared to the benzo(a)pyrene immortalized cells. However, total choline-containing metabolites and PCho levels were still less than those of tumor derived cells. *ErbB2* is an important (proto)oncogene which is amplified in 20-30% of breast cancer cases and is associated with poor prognosis; amplification of this oncogene is thought to occur late in tumor progression [25, 26, 30, 31]. Transformation of 184B5 by this gene results in the ability of these cells to form colonies in semi-solid medium, and to form small, low frequency tumors with high latency *in vivo* [32]. Our data with *erbB2* demonstrates a new and heretofore unknown metabolic role for *erbB2*, and supports the possibility that growth factor mediated activation of the tyrosine kinase cascade (involving receptor-*grb* 2-*sos*-*ras* - *raf*-1 - *MEK*-*MAPK*), can lead to an increase in PCho levels [33, 34]. In general, the levels and expression of receptors and proteins involved in the growth factor receptor-tyrosine kinase pathway tend to increase with malignancy. For instance, levels of epidermal growth factor receptor are low in the 184 strain, moderately high in 184A1, 184B5 and 184B5-*erbB2* cells, and very high in MDA-MB-231 cells [35, 36]. In addition, Daly *et al.* [37] reported upregulation of *grb2* mRNA/protein and the *ras* signaling pathway in MCF-7 and MDA-MB-231 cells compared to normal HMEC.

All of the breast tumor cell lines showed the GPC to PCho switch. In addition to this switch, all breast tumor cells showed significantly higher total choline-containing metabolite levels ( $p < 0.05$ ). The increased total choline-containing metabolite levels, was mainly due to an increase in PCho levels and, to a lesser and variable extent, an increase in GPC levels. There was a gradual increase in both total choline-containing metabolite levels and PCho levels as cells the cells acquired malignant phenotype (normal < immortal < oncogene transformed < tumor derived) with the highly invasive metastatic cell lines showing the highest levels. The high total choline content in the tumorigenic cells may be related to the multiple genetic changes which are associated with the multistep process of carcinogenesis [26], and may explain the progressive ability of these cells to gain anchorage-independent growth, form primary tumors in immune compromised mice and finally to metastasize. Our studies confirm the work of Ting *et al.* [38], who showed for a limited number of cell lines, that levels of choline-containing metabolites were low in a normal mammary epithelial strain and high in two tumor-derived cell lines. Our results also support recent clinical observations that the total choline peak is higher for malignant lesions than for benign ones [39].

It has been postulated that the rapid growth and proliferation of cancer cells and increased membrane/fatty acid requirements may be responsible for the high choline phospholipid metabolite levels in cancer versus normal tissues; the same argument could be made for benign lesions versus invasive cancers. However, the data presented here and that of Ting *et al.* [38] show that choline-containing metabolite levels remain low in normal HMEC in culture when the cells are proliferating at approximately similar rates as tumor derived cells, and suggest that although proliferation related changes may occur, rate of proliferation *per se* cannot completely account for the increased choline phospholipid metabolism. In this study we have demonstrated that an alteration in MCPM is linked to malignant transformation and progression of mammary epithelium. Currently, the exact mechanisms underlying the altered metabolism are unknown. Possible mechanisms include, activation of enzymes involved in MCPM such as via enhanced receptor tyrosine kinase cascade or differential induction of choline kinase isozymes as previously reported for carcinogen-treated rat liver. Other possible mechanisms which need to be investigated include amplification of choline kinase, phospholipase C, phospholipase D and phospholipase A genes during carcinogenesis.

## STUDY 2. 3D IMAGING AND HISTOLOGICAL STUDIES OF SOLID HUMAN BREAST CANCER MODELS

### EXPERIMENTAL METHODS

Imaging studies were performed on a GE Omega 4.7T instrument with a solenoidal coil placed around the tumor (volumes 100-300mm<sup>3</sup>) for human breast cancer models MCF-7, MDA-MB-231 and MDA-MB-435 inoculated in the mammary fat pad or flank of SCID mice. The tail vein of the anesthetized animal was catheterized before it was placed in the magnet. Animal body temperature was maintained at 37°C by heat generated from a warm water pad. Multi-slice relaxation rates ( $T_1^{-1}$ ) in tumors were obtained by a saturation recovery method combined with fast T<sub>1</sub> SNAPSHOT-FLASH

imaging (flip angle of  $70^\circ$ , echo time of 2ms). Images of 8 slices (slice thickness of 1mm) acquired with an in-plane spatial resolution of  $250\mu\text{m}$  ( $64 \times 64$  matrix, 16mm field of view, NS=16) were obtained for 3 relaxation delays (100ms, 500ms, and 1s) for each of the slices. Thus,  $64 \times 64 \times 8$   $T_1$  maps were acquired within 7 minutes. An  $M_0$  map with a recovery delay of 7s was acquired once at the beginning of the experiment. Images were obtained before i.v. administration of 0.2ml of 60 mg/ml albumin-GdDTPA in saline (dose of 500mg/kg) and repeated every 8 minutes, starting 10 minutes after the injection, up to 32 minutes. Relaxation maps were reconstructed from data sets for three different relaxation times and the  $M_0$  data set. At the end of the imaging studies, the animal was sacrificed, 0.5 ml of blood was withdrawn from the inferior vena cava, and tumors were marked for referencing to the MRI images, excised, and fixed in 10% formalin for sectioning and staining.

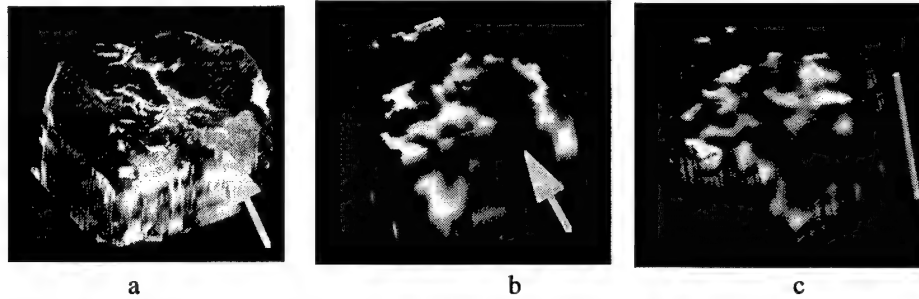
Vascular volume and permeability product surface area (PS) maps were generated from the ratio of  $\Delta(1/T_1)$  values in the images to that of blood. The slope of  $\Delta(1/T_1)$  ratios versus time in each pixel was used to compute (PS) while the intercept of the line at zero time was used to compute vascular volume. Thus, vascular volumes were corrected for permeability of the vessels. Ten  $5\mu\text{m}$  thick histological sections obtained at  $500\mu\text{m}$  intervals through the tumor were stained with hematoxylin eosin. Sections were digitized with a Sanyo CCD camera attached to an optical microscope.

3-D reconstruction of both MRI and histological sections was performed using the Clinical Microscope Visualization software that we are developing as a research tool for use in our investigation. The software consists of two parts, the first part forms the volume image from 2-D images and the second part performs visualization of the volumetric model in suitable 3-D perspective. The high resolution image 'tiles' representing the histological sections acquired from the microscope are stitched along the overlapping borders to produce a large 'virtual' field of view image that represents the full cross section which could not be acquired otherwise in a single actual field of view at the selected high resolution. Such a virtual field of view image can be panned around, zoomed in, to look at selected regions at the full resolution in which they are acquired. Each cross-section is then layered one over the other, to compose the 3-D volume. The volume image is then interactively rendered using the volumetric visualization software, to adjust the transfer functions that control the voxel transparency and intensity characteristics of various structures of interest, to delineate it from the surrounding structures. The software system is developed around Silicon Graphics Inc., Workstation systems, taking full advantage of the hardware accelerated graphics capabilities such as 2- and 3- D Textures to provide interactive rendering results.

## RESULTS AND DISCUSSION

We observed areas of low vascular volume to correspond spatially with necrotic areas (shown by arrows in a and b in Figure 5). As observed before, regions with high

vascular volume did not coincide spatially with regions of high permeability (arrow in c, Figure 5) although there was some overlap. The non-uniform edges for the 3-D reconstructed histological map were due to slight deformation during sectioning of the tumor in some of the sections. We have shown here, for the first time, the feasibility of obtaining 3-D maps of histological morphology to interactively relate to noninvasive quantitative 3-D maps of tumor vascular volume and permeability. The results obtained confirm our earlier hypothesis that low vascular volume is associated with areas containing dying zones of cells.



**Figure 5:** 3-D reconstructed maps of histological morphology (a), vascular volume (b) and vascular permeability (c) obtained using our Clinical Microscope Visualization software. Areas of low vascular volume correspond spatially with necrotic areas (shown by arrows in a and b).

The interactive ability of the software program (demonstrable on video) allows zooming into regions of interest as well as simultaneous volumetric visualization across multiple 3-D maps. Thus a region of interest placed on a necrotic area or an area with high VEGF expression is immediately displayed on the corresponding vascular volume or permeability map or *vice versa*. To understand the development and role of tumor vascular architecture in the growth and dissemination of solid tumors it is frequently necessary to examine the relationship between information which may only be obtained following histological sectioning, such as the distribution of VEGF expression or presence of necrotic areas, to information obtained noninvasively with MRI such as vascular volume or permeability. With single slice 2-Dimensional (2-D) information, valuable details about developmental patterns of structures of interest for planes other than the cross sectional one are lost since it is difficult to visually and mentally piece together such information, even when multiple cross-sectional slices are obtained. Here for the first time we obtained 3-Dimensional (3-D) reconstructed histopathological maps demonstrating a spatial relationship between functionality of vasculature obtained in 3-D reconstructed maps of vascular volume and permeability and histological morphology. These technological advances will play a unique role in understanding tumor pathophysiology and allowing us to accomplish our research goals.

## CONCLUSIONS

The major findings to emerge from the studies performed for year 2 are:

- Choline phospholipid metabolite levels progressively increase in cultured HMEC as cells become more malignant. We therefore propose that carcinogenesis in human breast epithelial cells results in progressive alteration of membrane choline phospholipid metabolism. This work is relevant to diagnosis of breast cancer and also provides a rationale for selective pharmacological intervention.
- Lactate levels increase significantly in cultured HMEC following malignant transformation. However, following malignant transformation, there did not appear to be a close dependence between lactate levels observed in malignant cell lines and the metastatic potential of these lines. The increased lactate production may result in an acidic environment which may promote invasive behavior and contribute to metastasis.
- 3-dimensional interactive analysis of vascular volume and permeability and histological morphology demonstrates that areas of low vascular volume are associated with cell death and increasingly permeable vasculature.

## REFERENCES

1. Folkman, J., Watson, K., Ingber, D. and Hanahan, D., Induction of angiogenesis during the transition from hyperplasia to neoplasia. *Nature* **339**, 58-61 (1989).
2. Liotta, L.A., Steeg, P.S., Stetler-Stevenson, W.G., Cancer metastases and angiogenesis: an imbalance of positive and negative regulation. *Cell* **64**, 327-336 (1991).
3. Liotta, L., J. Kleinerman, and G. Saidel, Quantitative relationships of intravascular tumor cells, tumor vessels and pulmonary metastases following tumor implantation. *Cancer Research* **34**, 997-1004 (1974).
4. Folkman, J., The vascularization of tumors. *Scientific American* **234**, 59-73 (1976).
5. Folkman, J., How is blood vessel growth regulated in normal and neoplastic tissue ? *Cancer Research* **46**, 467-473 (1986).
6. Moses, M.A., The role of vascularization in tumor metastasis, in "Microcirculation in cancer metastasis", F. William Orr Buchanan, M.R., Weiss, L., Eds. 1991, CRC Press: p. 257-276.
7. Weidner, N., Semple, J.P., Welch, W.R. and Folkman, J., Tumor angiogenesis and metastasis - correlation in invasive breast carcinoma. *New England Journal of Medicine* **324**, 1-8 (1991).
8. Horak, E.R., Leek, R., Klenk, N., LeJeune, S., Smith, K., Stuart, N., Greenal, M., Stepniewska, K. and Harris, A.L. , Angiogenesis, assessed by platelet/endothelial cell adhesion molecule antibodies, as indicator of node metastases and survival in breast cancer. *Lancet* **340**, 1120-1124 (1992).
9. Mareel, M.M., Baetselier, P., van Roy, F.M., Mechanisms of Invasion and Metastasis. 1991, CRC Press.
10. Shweiki, D., Itin, A., Soffer, D. and Kesbet, E., Vascular endothelial growth factor induced by hypoxia may mediate hypoxia-initiated angiogenesis. *Nature* **359**, 843-845 (1992).
11. Plate, K.H., Breier, Weich, H. and Risau, W., Vascular endothelial growth factor is a potential tumor angiogenesis facotr in human gliomas in vivo. *Nature* **359**, 845-848 (1992).
12. Cooper, R.G., Taylor, C.M., Choo, J.J. and Weiss, J.B., Elevated endothelial-cell stimulating angiogenic factor activity in rodent glycolytic skeletal muscles. *Clinical Science* **81**, 267-270 (1991).

13. Knighton, D.R., Hunt, T.K., Scheuenstuhl, H. and Banda, M., Oxygen tension regulates the expression of angiogenesis factor by macrophages. *Science* **221**, 1283-1285 (1983).
14. Knighton, D., Schummerth, S., and Fiegel, V., Environmental regulation of macrophage angiogenesis., in "Current Communications in Molecular Biology, Angiogenesis: Mechanisms in Pathobiology.", D.B. Rifkin Klagsbrun, M., Eds. 1987, Cold Spring Harbor Laboratory: p. 150-157.
15. Jensen, A.J., Hunt, B., Scheuenstuhl, B. and Banda, M.J., Effect of lactate, pyruvate and pH on secretion of angiogenesis and mitogenesis factors by macrophages. *Laboratory Investigations* **56**, 574-578 (1986).
16. Rozhin, J., Sameni, M., Ziegler, G. and Sloane, B.F., Pericellular pH affects distribution and secretion of Cathepsin B in Malignant cells. *Cancer Research* **54**, 6517-6525 (1994).
17. Kato, Y., Nakayama, Y., Umeda, M. and Miyazaka, K., Induction of 103kDa gelatinase/type IV collagenase by acidic culture conditions in mouse metastatic melanoma cell lines. *J. Biol. Chem.* **267**, 11424-11430 (1992).
18. Plumb, J.A., Milroy, R., Kaye, S. B., Effects of pH dependence of 3-(4,5-Dimethylthiazole-2-yl)-2,5-diphenyltetrazolium bromide-formazan absorption on chemosensitivity determined by a novel tetrazolium-based assay. *Cancer Research* **49**, 4435-4440 (1989).
19. Schwickert, G., Walenta, S., Sundfor, K., Rofstad, E.K. and Mueller-Klieser, W., Correlation of high lactate levels in Human Cervical Cancer with Incidence of Metastasis. *Cancer Research* **55**, 4757-4759 (1995).
20. Schlappack, O.K., Zimmerman, A. and Hill, R.P., Glucose starvation and acidosis: effect on experimental metastatic potential, DNA content and MTX resistance of murine tumour cells. *British Journal of Cancer* **63**, 692-700 (1991).
21. Young, S.D., Marshall, R.S. and Hill, R.P., Hypoxia induces DNA overreplication and enhances metastatic potential of murine tumor cells. *Proc. Natl. Acad. Sci. USA* **85**, 9533-9537 (1988).
22. Ruiz-Cabello, J. and J.S. Cohen, Phospholipid metabolites as indicators of cancer cell function. (1992).
23. Negendank, W., Studies of human tumors by MRS: a review. *NMR Biomed.* **5**, 303-324 (1992).
24. Smith, T.A.D., Eccles, S., Ormerod, M.G., Tombs, A.J., Titley, J.C. and Leach, M.O., The phosphocholine and glycerophosphocholine content of an iestrogen-sensitive rat

mammary tumour correlates strongly with growth rate. *British Journal of Cancer* **64**, 821-826 (1991).

25. Dickson, R.B., Salamon, D. S., Lippman, M. E., Tyrosine kinase receptor-nuclear protooncogene interaction in breast cancer. *Cancer Treat. Res.* **61**, 249-273 (1992).

26. Beckman, M.W., Niederacher, D., Schnurch, H. G., Guesterson, B. A., Bender, H. G., Multistep carcinogenesis of breast cancer and tumor heterogeneity. *J. Mol. Med.* **1997**, 429-437 (1993).

27. Stampfer, M.R., Bartley, J. C., Induction of transformation in continuous cell lines from normal human mammary epithelial cells. *Proc. Natl. Acad. Sci. USA* **82**, 2394-2398 (1985).

28. Thompson, E.W., Torri, J., Sabol, M., Sommers, C. L., Byers, S., Valverius, E. M., Martin, G. R., Lippman, M. E., Stampfer, M.R., Dickson, R. B., Oncogene-induced basement membrane invasiveness in human mammary epithelial cells. *Clin. Exp. Metastasis* **12**, 181-194 (1994).

29. Stampfer, M.R., Bodnar, A., Garbe, J., Wong, M., Pan, A., Villeponteau, B., Yaswen, P., Gradual phenotypic conversion associated with immortalization of cultured human mammary epithelial cells. *Mol. Biol. Cell* **8**, 2391-2405 (1997).

30. Adnane, J., Gaudray, P., Simon\_lafontaine, J., Jeanteur, P., Theillet, C., Proto-oncogene amplification and breast cancer phenotype. *Oncogene* **4**, 1389-1395 (1989).

31. Slamon, D.J., Clark, G. M., Wong, S. G., Levin, W. J., Ulrich, A., McGuire, W. L., Human breast cancer: correlation of relapse and survival with amplification of the HER-2/neu oncogene. *Science* **235**, 177-182 (1987).

32. Pierce, J.H., Arnstein, P., DiMarco, E., Artrip, J., Kraus, M. H., Lonardo, F., DiFiore, P. P., Aaronson, S. A., Oncogenic potential of erbB-2 in human mammary epithelial cells. *Oncogene* **6**, 1189-1194 (1991).

33. Cai, H., Erhardt, P., Troppmair, J., Diaz-Meco, M.T., Sithanandam, G., Rapp, U. R., Moscat, J., Cooper, G. M., Hydrolysis of phosphatidylcholine couples Ras to activation of Raf protein kinase during mitogenic signal transduction. *Mol. Cell Biol.* **13**, 7645-7651 (1993).

34. Ratnam, S., Kent, C., Early increase in choline kinase activity upon induction of the H-ras oncogene in mouse fibroblast cell lines. *Arch. Biochem. Biophys.* **323**, 313-322 (1995).

35. Smith, L.M., Birrer, M. J., Stampfer, M. R., Brown, P. H., Breast cancer cells have lower activating protein 1 transcription factor activity than normal mammary epithelial cells. *Cancer Res.* **57**, 3046-3054 (1997).

36. de Cremoux, P., Gauville, C., Closson, V., Linares, G., Calvo, F., Tavitian, A., Olofsson, B., EGF modulation of the ras-related rhoB gene expression in human breast cancer cell lines. *Int. J. Cancer* **59**, 408-415 (1994).
37. Daly, R.J., Binder, M. D., Sutherland, R. L., Overexpression of the Grb gene in human breast cancer cell lines. *Oncogene* **9**, 2733-2727 (1994).
38. Ting, Y.-L., Sherr, D., Degani, H., Variations in energy and phospholipid metabolism in normal and cancer human mammary epithelial cells. *Anticancer Research* **16**, 1381-1388 (1996).
39. Mackinnon, W.B., Barry, P. A., Malycha, P. L., Gillett, D. L., Russell, P., Lean, C. L., Doran, S. T., Barraclough, B. H., Bilous, M., Mountford, C., Fine-needle biopsy specimens of benign breast lesions distinguished from invasive cancer ex viv with proton MR spectroscopy. *Radiology* **204**, 661-667 (1997).